JOURNAL OF NEUROTRAUMA 29:1469–1482 (May 1, 2012)

DOI: 10.1089/neu.2011.2161

Preventing Flow-Metabolism Uncoupling Acutely Reduces Axonal Injury after Traumatic Brain Injury

Neil G. Harris,[1] Yevgeniya A. Mironova,[1] Szu-Fu Chen,[2,3] Hugh K. Richards,[4,5] and John D. Pickard,[4,5]

Abstract

We have previously presented evidence that the development of secondary traumatic axonal injury is related to the degree of local cerebral blood flow (LCBF) and flow-metabolism uncoupling. We have now tested the hypothesis that augmenting LCBF in the acute stages after brain injury prevents further axonal injury. Data were acquired from rats with or without acetazolamide (ACZ) that was administered immediately following controlled cortical impact injury to increase cortical LCBF. Local cerebral metabolic rate for glucose (LCMRglc) and LCBF measurements were obtained 3 h post-trauma in the same rat via ^{18}F-fluorodeoxyglucose and ^{14}C-iodoantipyrine co-registered autoradiographic images, and compared to the density of damaged axonal profiles in adjacent sections, and in additional groups at 24 h used to assess different populations of injured axons stereologically. ACZ treatment significantly and globally elevated LCBF twofold above untreated-injured rats at 3 h ($p < 0.05$), but did not significantly affect LCMRglc. As a result, ipsilateral LCMRglc:LCBF ratios were reduced by twofold to sham-control levels, and the density of β-APP-stained axons at 24 h was significantly reduced in most brain regions compared to the untreated-injured group ($p < 0.01$). Furthermore, early LCBF augmentation prevented the injury-associated increase in the number of stained axons from 3–24 h. Additional robust stereological analysis of impaired axonal transport and neurofilament compaction in the corpus callosum and cingulum underlying the injury core confirmed the amelioration of β-APP axon density, and showed a trend, but no significant effect, on RMO14-positive axons. These data underline the importance of maintaining flow-metabolism coupling immediately after injury in order to prevent further axonal injury, in at least one population of injured axons.

Key words: autoradiography; blood flow; cortical contusion injury; glucose metabolism; uncoupling

Introduction

Clinical and experimental studies have demonstrated that axonal injury is responsible for much of the morbidity and mortality associated with traumatic brain injury (TBI) (Adams et al., 1989; Christman et al., 1994; Grady et al., 1993; Maxwell et al., 1993,1997). While it was once thought that traumatically injured axons are mechanically severed at the time of injury, it is now known that primary axotomy rarely occurs (Maxwell et al., 1997), at least after lateral fluid percussion injury (Singleton et al., 2002). Rather, in the majority of cases, the primary mechanical insult provokes secondary biochemical processes involving a transient, focal disruption of the axolemma allowing for calcium influx and the initiation of an enzyme cascade resulting in further damage (Maxwell et al., 1995,1999; Pettus and Povlishock, 1996). The resulting mitochondrial swelling and/or injury and disruption of axoplasmic transport can ultimately lead to disconnection of swollen axons from their distal segment (Buki et al., 1999b,2000; Maxwell et al., 1997; Okonkwo et al., 1998), with either cell death, or simply neuronal atrophy in more mild types of injury (Greer et al., 2011). While it is known that the process of traumatic axonal injury (TAI) evolves over a relatively long time course before axotomy occurs (Maxwell et al., 1997), the mechanisms involved are not well understood. Previous work has focused on the

[1]University of California–Los Angeles Brain Injury Research Center, Department of Neurosurgery, University of California, Los Angeles, California.
[2]Department of Physical Medicine and Rehabilitation, Cheng Hsin General Hospital, Taipei, Taiwan.
[3]Department of Physiology, National Defense Medical Center, Taipei, Taiwan.
[4]Academic Neurosurgery, Centre for Brain Repair, University of Cambridge, Cambridge, United Kingdom.
[5]Wolfson Brain Imaging Centre, University of Cambridge, Cambridge, United Kingdom.

intermediate events that lead to TAI, such as mitochondrial failure (Buki et al., 1999a,2000), and the downstream consequence of Ca^{2+} influx in terms of calpain activation (Buki et al., 1999b; Saatman et al., 1996,2003). Relatively little consideration has been directed toward upstream pathophysiological events such as circulatory and metabolic dysfunction and their overall influence on the fate of damaged axons.

Regional or global alterations in cerebral blood flow (CBF) have been reported after both clinical (Bouma and Muizelaar 1992; Bouma et al., 1991; Coles et al., 2002; Marion and White, 1991; Martin et al., 1997; Robertson et al., 1992) and experimental brain injury (Bryan et al., 1995; Forbes et al., 1997; Kochanek et al., 1995; Richards et al., 2001; Yamakami and McIntosh 1991), although the early reductions in CBF typically tend to lie above the threshold classically associated with ischemic brain injury. A number of studies have demonstrated acute elevations in local cerebral glucose consumption after clinical (Bergsneider et al., 1997) and experimental brain injury (Sunami et al., 1989; Sutton et al., 1994; Richards et al., 2001; Yoshino et al., 1991), representing raised metabolic demand. In previous work we have described a state of marked, region-specific uncoupling of local cerebral metabolic rate for glucose (LCMRglc) and local cerebral blood flow (LCBF) at 3 h after cortical contusion injury (Chen et al., 2004). The degree of uncoupling and LCBF reduction in white matter regions were strongly associated with the development of axonal injury, indicating that secondary damage occurs in brain regions that are subjected to an energy demand disproportionate to their level of local perfusion. It is plausible, therefore, that preserving the coupling between blood flow and metabolism, and/or reversing possible traumatic vasospasm will interrupt the injury cascade and prevent axotomy by relieving the local bioenergetic stress that likely contributes to the development of axonal injury. We use the term "uncoupled" throughout this article to infer an altered LCBF:LCMRglc ratio in the brain during baseline neuronal activity in the same way that the term "mismatch" is used in the literature. However, we do not imply that these parameters necessarily remain coupled during neuronal activation.

The aim of this study was to test the hypothesis that augmenting LCBF in the acute stages after brain injury results in an improved balance between LCBF and metabolic demand so that, consequently, axonal injury is reduced at later time points. To achieve this, LCBF was increased using acetazolamide (ACZ), a selective inhibitor of carbonic anhydrase that increases LCBF via local tissue acidosis (Bickler et al., 1988). Axonal injury was assessed through the use of β-amyloid precursor protein (β-APP)-immunostained profiles, since axonal accumulation of β-APP is recognized to be a sensitive marker of traumatically induced axonal damage (Gentleman et al., 1993; Stone et al., 2000). There is good evidence to suggest that neurofilament compaction represents a different population of damaged axons, and does not overlap with impaired axonal transport in both neonatal and mature rodent nervous systems (Marmarou et al., 2005; Stone et al., 2004). Therefore, additional experiments were performed for stereologic assessment of both impaired axon transport and neurofilament compaction in order to provide a more comprehensive and robust analysis of any treatment effects among these different populations of injured axons. We confined these measurements to the corpus callosum, since we have previously found that intra- and interhemispheric connectivity is severely disrupted within this region in this model (Harris et al., 2009). As such, any positive effects of treatment within this region might potentially confer considerable functional benefits.

Methods

Experimental protocol

Acetazolamide (ACZ, 150 mg kg^{-1} in normal saline IP) or vehicle was administered immediately after injury followed by either: [1] laser Doppler analysis of cortical blood flow at 1–3 h post-injury to validate the ACZ-induced reduction in perfusion ($n = 3$/group); [2] dual-labeled LCBF and LCMRglc autoradiographic measurements together with immunohistochemistry on adjacent sections for the early axonal injury marker β-APP at 3 h ($n = 6$/group); [3] β-APP immunohistochemistry staining at 24 h to determine the longer-term fate of injured neurones ($n = 6$); or [4] unbiased stereological analysis of both β-APP and neurofilament compaction (via RM014 immunostaining) at 24 h after injury ($n = 8$ and 6/group in the ACZ and saline-vehicle groups, respectively).

In the interest of local animal-use policies that encourage reduction of the number of animals used for experimentation, the effect of treatment in studies 2 and 3 was determined by comparison to prior data (Chen et al., 2004) from untreated injured rats at 3 h and 24 h after injury, and from sham-operated rats ($n = 6$/ group). Importantly, with the exception of the stereologic data (Fig. 7), all surgeries, quantification of all autoradiographic data (Figs. 3–5), and β-APP data acquisition (Fig. 6) from ACZ-treated rats reported here were accomplished concurrently with previous data acquired from injured and sham-injured rats. Thus, although some sham/injury data are reused here, the interleaved fashion with which all group data were originally acquired makes them appropriate control groups and ensures that statistical comparisons are valid. All stereologic data (Fig. 7) were newly acquired and were not compared to any prior control data.

Surgical procedures

All study protocols were approved by the United Kingdom Animals Scientific Procedures Act, 1986, and by the University of California–Los Angeles (UCLA) Chancellor's Animal Research Committee, and the Public Health Service Policy on Humane Care and Use of Laboratory Animals. Cannulae were inserted into the left femoral artery and right femoral vein of male Sprague-Dawley rats (261 ± 6 g body weight) anesthetized with 2% isofluorane in O_2 flowing at 0.8 L/min. The method for induction of cortical contusion impact (CCI) injury was performed in the manner previously described (Chen et al., 2003,2004). Briefly, following reduction of anesthesia to 1–1.5% isofluorane and 0.8/0.4 L/min N_2O/O_2, a 2.5-mm-diameter piston was advanced through a 5-mm craniotomy (0.5 mm posterior to the coronal suture and 3 mm left-lateral to the sagittal suture) and onto the brain at 4 m/sec to a deformation depth of 2 mm below the dura. The bone flap was immediately replaced and sealed and the scalp was sutured closed. In the 24-h survival group, the rats were placed in a heated cage to maintain body temperature while recovering from anesthesia, and soluble paracetamol (1 mg/mL; Cox Pharmaceuticals, Barnstaple, Devon, U.K.) was administered in the drinking water post-operatively. Rats in the 3-h

Table 1. Physiological Data Before and After Injection of 150 mg/kg Acetazolamide

Variable	*Before injection*	*After injection (2 h)*
Po_2 (mm Hg)	130 ± 1.4	128 ± 1.7
Pco_2 (mm Hg)	39 ± 0.6	59 ± 1.3†
Plasma glucose (mg/dL)	108 ± 3.5	114 ± 3.3

†$p < 0.05$.
Values are mean ± standard error of the mean.
Pco_2, partial carbon dioxide pressure; Po_2, partial oxygen pressure.

survival group were maintained under anesthesia until the termination of the experiment. Blood gases and plasma glucose were measured before and 2 h after treatment (Table 1). Body temperature was monitored throughout surgery by a rectal probe and maintained at 37.0 ± 0.5°C using a heated pad (Harvard Apparatus Ltd., Edenbridge, Kent, U.K.).

Validation of the CBF response to acetazolamide

The ACZ-induced rise in LCBF was validated in a another group of injured rats ($n = 6$) by laser Doppler flowmetry. The purpose was twofold: to determine the optimal dose of ACZ to produce a significant rise in LCBF, and to determine the dose that would ensure a sustained increase for at least 3 h. Immediately after injury, the rats were positioned in a stereotaxic frame and a small burr hole was made in the skull over the homologous parietal cortex, contralateral to the center of the contusion. A laser Doppler probe (needle-shaped, 0.8 mm; Moore Instruments, Axminster, Devon, U.K.) mounted on a micromanipulator was used to monitor LCBF. Care was taken to obtain flow readings only from areas free of large pial vessels. After stabilizing LCBF, the animals were given intraperitoneal ACZ (Wyeth, Madison, NJ) at 100 mg/kg^{-1} ($n = 3$), or 150 mg/kg^{-1} ($n = 3$), and LCBF and arterial blood pressure were continuously monitored for 3 h.

LCMRglc and LCBF by autoradiography

The procedures used to determine LCMRglc and LCBF were the same as previously described (Chen et al., 2004). Briefly, 30 MBq of ^{18}F-fluorodeoxyglucose (FDG; ~0.5 mL) was injected into the femoral vein 2 h and 15 min after the injury, and timed arterial samples (50 μL) were collected over 45 min through the catheterized femoral artery into microcapillary tubes. After collection of the last arterial sample at 3 h after injury, 925 KBq of ^{14}C- iodoantipyrine (^{14}C-IAP; Tocris Cookson, Bristol, U.K.) was infused intravenously over 60 sec using a ramped infusion, and arterial blood samples were collected onto filter paper every 3 sec. Following decapitation, the brain was rapidly excised, frozen in dry ice-cooled isopentane, and subsequently sectioned at 20 μm in a cryostat. Brain and plasma ^{18}FDG and ^{14}C-IAP concentrations were determined using a phosphor-imager (Cyclone; PerkinElmer Life Sciences Ltd., Cambridge, U.K.) as described previously (Chen et al., 2004).

Image analysis

Region-of-interest (ROI) data were obtained from LCMRglc and LCBF images that were co-registered using a mutual information algorithm implemented as previously described (Chen et al., 2004). ROIs were anatomically defined on adjacent, co-registered, cresyl violet-stained sections at the level −2.80 mm from the bregma within the following brain regions: contusion core, contusion margin, CA1, CA3, dentate gyrus, dorsal thalamus, cingulum, corpus callosum, external capsule, and internal capsule (Fig. 1). LCMRglc values were determined using the operational equation using appropriate K_1, K_2, and K_3 values for FDG: respectively, 0.33, 0.76, and 0.14 min^{-1} for grey matter, and 0.15, 0.40, and 0.04 min^{-1} for white matter (Ingvar et al., 1991). A lumped constant of 0.6 was used (Lear and Ackermann, 1989).

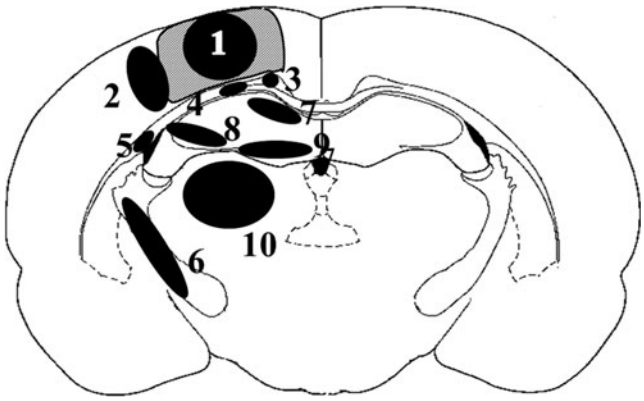

FIG. 1. A brain atlas coronal section (Paxinos and Watson, 1997) illustrating the core contused region (hatched area) at −2.80 mm to the bregma. Measurements for LCMRglc and LCBF and the density of β-APP-immunoreactive profiles were determined in the following regions of interest: (1) contusion core, (2) pericontusion margin, (3) cingulum, (4) corpus callosum, (5) external capsule, (6) internal capsule, (7) CA1, (8) CA3, (9) dentate gyrus, and (10) dorsolateral thalamus (LCBF, local cerebral blood flow; LCMRglc, local cerebral metabolic rate for glucose; β-APP, β-amyloid precursor protein).

Immunohistochemistry

Frozen sections adjacent to the autoradiographically-analyzed sections at 3 h and the corresponding sections from brains at 24 h not used for autoradiography were processed for immunohistochemistry using rabbit anti-β-APP C-terminus polyclonal antibody (1:500; Zymed Laboratories, San Francisco, CA). To ensure antibody specificity, the primary antibody was omitted in control studies. Sections were quenched with 3% hydrogen peroxide in 10% methanol, blocked in 3% normal goat serum (NGS; Dako, Cambridge, U.K.) with 0.2% Triton X-100 and phosphate-buffered saline (TXTBS; Sigma-Aldrich, Poole, Dorset, U.K.), and incubated overnight at room temperature in the primary antibody in TXTBS containing 1% NGS. Primary antibody was detected using biotinylated secondary antibody (biotinylated anti-rabbit IgG) at a concentration of 1:200 in Trizma-buffered saline (TBS) with 1% NGS, followed by horseradish peroxidase-conjugated streptavidin (Dako). The enzyme reaction was visualized using diaminobenzidine (DAB; Dako).

Additional groups of rats for stereology were transcardially perfusion-fixed with saline followed by 4% paraformaldehyde at 24 h after injury. Brain sections were processed for

double immunofluorescence using anti-APP and anti-neurofilament M (RMO.14) antibody (Invitrogen, Carlsbad, CA). Briefly, coronal 50-μm sections 600-μm apart were incubated in 10 M sodium citrate buffer (pH 6.0) overnight at 4°C, and then heated in a water bath at 95°C 2×10 min with a 10-min cool down. The sections were then washed 3×5 min in phosphate-buffered saline (PBS), blocked with 10% NGS in PBS for 60 min, and co-incubated in primary antibodies (1:150 RMO14 and 1:500 APP with 5% NGS in PBS) overnight at room temperature on a shaker. On the following day, the sections were washed 3×5 min with PBS and co-incubated in secondary antibodies (1:500 goat anti-rabbit IgG Alexa-Fluor 488 and 1:500 goat anti-mouse IgG Alexa-Fluor 555 with 5% NGS in PBS) for 1 h. Finally, the sections were washed 3–5 min with PBS, mounted with mounting medium with DAPI, and the slides were sealed with nail polish. Prior to quantitative structural analysis, representative sections from each brain were examined under DAPI illumination and assessed for primary damage to the corpus callosum or cingulum. In order to analyze the same region of white matter by stereology in each brain, only brains in which the white matter was grossly intact and did not contain the contusion border were analyzed further.

Axonal pathology and contusion volume

Axon pathology was first quantified on β-APP-stained, frozen sections adjacent to the autoradiographically-analyzed sections at the level–2.80 mm from the bregma, using a light microscope interfaced with an image analysis system (Olympus computer assisted stereological toolbox-grid system; Olympus, Sikelborg, Denmark). Profiles were identified as dark brown, elongated, or circular processes of retraction balls/bulbs, or reactive processes as shown previously (Chen et al., 2004). The number of β-APP axonal profiles was counted at a magnification of $40\times$ on five randomly-positioned 276-μm^2 fields of view within those ROIs analyzed for LCMRglc and LCBF autoradiograms (Fig. 1).

In order to determine whether acute interventions to alter flow-metabolism coupling differentially affected injured axon populations, as determined by impaired axonal transport or neurofilament compaction, we used unbiased stereology to estimate the number of β-APP- and RMO-positive profiles at 24 h within the white matter underlying the contusion. The optical fractionator method (StereoInvestigator; MicroBrightfield, Williston,VT) was used to count either the number of single-labeled axons positive for β-APP, RMO, or β-APP/RMO double-labeled axons under epifluorescent illumination. β-APP-positive profiles were identified as elongated or circular processes of retraction balls/bulbs. RMO14-positive profiles were identified as thin and elongated, or displaying vacuolization. Counts were performed using a 150×150-μm counting grid at $400\times$ magnification, on 5 sections/brain, 600-μm apart, between 2 and -2 mm from the bregma, within the ipsilateral corpus callosum and cingulum that was outlined under DAPI illumination as a single ROI on each section from the midline to the level of the rhinal fissure ventrolaterally. Axon profile counts were then made within the contour at wavelengths specific for β-APP and RMO fluorophore-tagged illumination (Fig. 7A–E). An estimate of the volume of cortical grey and white matter tissue loss was made by contouring the outline of the remaining ipsilateral versus contralateral cortical grey matter and underlying corpus callosum, from the midline to the rhinal fissure on all sections analyzed for axon pathology using DAPI-stained sections. The volume of tissue remaining was estimated on each cortical hemisphere by summing the contoured areas, and multiplying by the distance between sections. The amount of ipsilateral cortical volume loss was then calculated as the cortical volume difference between hemispheres, expressed as a percentage of contralateral cortical volume.

Statistical analysis

Physiological variables were compared before and after ACZ administration using a paired test. Cerebrovascular laser-Doppler post-injection LCBF data were tested for a group-level difference using a two-way repeated-measures analysis of variance (ANOVA). For all autoradiographic ROI parameters measured, differences between ACZ-treated, untreated-injured, and sham-control groups were tested for with a one-way ANOVA and corrected for multiple comparisons using the False Discovery Rate (FDR) approach (Benjamini and Hochberg, 1995; Chen et al., 2004). Herein, when significance was reached with the FDR, we have quoted the original probability levels that were obtained by the *t*-test ($p<0.05$, 0.01, 0.001). Autoradiographic data are graphically represented by normalization to sham-control values, and the absolute values for all groups are shown in Table 2, although for clarity and space, contralateral values are not shown for any group. An unpaired *t*-test was used to test for differences for all stereology data, after confirming original pilot data that predicted a greater than nominal 80% statistical power for determining group differences.

Results

Acetazolamide increases cortical LCBF for > 3 h

We first investigated a suitable dose of ACZ for increasing LCBF for a sustained period. Using laser Doppler flowmetry, we monitored LCBF contralateral to the injury site before, during, and after ACZ administration. We found that a higher dose (150 mg/kg^{-1}) produced a sustained increase in LCBF, to 237 ± 24% above baseline between 1 and 2 h after injection, which remained around 200% of baseline until 3 h (Fig. 2, $p<0.05$). In comparison, a lower dose (100 mg/kg^{-1}) had very little effect, resulting in only a 10% increase in the first 2 h, and returning to normal by 3 h. Therefore the higher ACZ dose was used in all further studies. As expected, ACZ treatment significantly increased blood Pco_2, but had no other effect on the measured blood physiological parameters (Table 1) or on arterial blood pressure (125 ± 4 versus 119 ± 4 mm Hg before and after injection, respectively).

Acetazolamide increases LCBF globally after injury

We next investigated the effect of ACZ on LCBF more globally using autoradiography. We found that acute administration of ACZ resulted in a profound effect on both grey and white matter LCBF (Fig. 3A and B). The decrease in ipsilateral LCBF normally associated with injury was significantly attenuated by ACZ administration; there was a global increase in LCBF above untreated-injured group values when measured at 3 h after injury (Fig. 3A–C; Table 2). Ipsilateral

TABLE 2. LCBF, LCMRGLC, AND LCMRGLC:LCBF ROI DATA FROM THE IPSILATERAL HEMISPHERE

	Core	*Marg*	*CA1*	*CA3*	*DG*	*Thal*	*Cing*	*CC*	*EC*	*IC*
LCBF (mL/100 g^{-1} min^{-1})										
Sham	85.6±1.3	112.7±2.4	98.6±3.6	102.4±2.5	115.4±1.9	147.4±2.2	87.1±2.0	54.5±2.9	73.1±0.6	81.9±1.4
Untreated	26.0±3.0	47.0±0.9	50.0±1.6	55.6±1.5	59.4±1.8	71.4±3.0	29.6±1.3	39.4±2.7	61.8±0.7	70.8±0.8
ACZ	38.8±3.6	*116.8±4.9	101.6±2.6	96.8±3.4	*129.6±2.6	*170.4±3.2	62.2±2.7	*61.2±2.9	101.8±1.6	*106.0±2.4
LCMRglc (μmol/100 g^{-1} min^{-1})										
Sham	74.8±3.2	65.3±5.9	63.8±8.7	63.0±6.2	60.7±4.7	83.9±5.5	60.0±4.8	49.0±7.1	63.4±1.4	47.2±3.4
Untreated	37.2±7.3	85.6±2.3	77.1±3.8	79.5±3.6	73.0±4.4	75.9±7.4	64.0±3.3	67.8±6.5	59.2±1.8	55.1±2.0
ACZ	38.8±8.9	72.8±11.9	59.2±6.3	60.3±8.4	59.7±6.3	65.6±7.8	55.1±6.7	48.8±7.1	48.7±3.9	50.1±5.9
LCMRglc:LCBF (μmol/mL^{-1})										
Sham	1.0±0.04	0.7±0.08	0.6±0.08	0.5±0.04	0.5±0.04	0.4±0.12	0.8±0.08	0.8±0.16	0.7±0.04	0.5±0.04
Untreated	1.5±0.37	2.6±1.06	1.5±0.20	1.8±0.45	1.7±0.33	1.3±0.20	2.5±0.41	1.7±0.16	1.1±0.12	0.6±0.08
ACZ	1.1±0.33	**0.7±0.16	**0.6±0.08	0.8±0.20	*0.5±0.04	*0.5±0.12	*1.0±0.16	*0.9±0.20	*0.6±0.08	0.5±0.04

Values are mean ± standard error of the mean.
*$p < 0.05$; **$p < 0.01$. ROI, region-of-interest; LCBF, local cerebral blood flow; LCMRglc, local metabolic rate for glucose; LCMRglc:LCBF, metabolism:flow ratio; ACZ, acetazolamide; DG, dentate gyrus; Thal, thalamus; Cing, cingulum; CC, corpus callosum; EC, external capsule; IC, internal capsule.

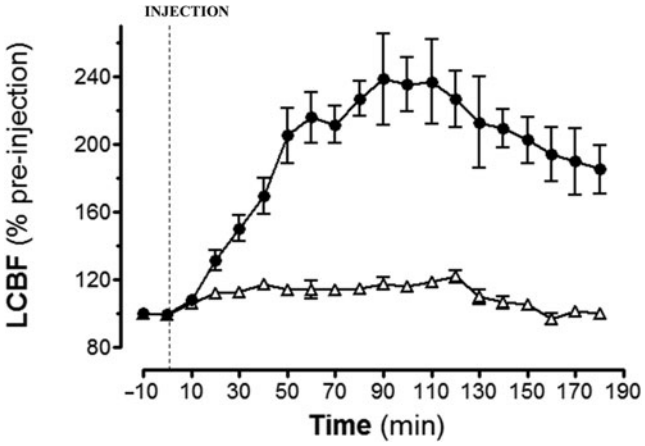

FIG. 2. Laser Doppler flow measurements of local cerebral blood flow (LCBF) over the contralateral parietal cortex immediately after injury, before, and after injection of acetazolamide (100 mg/kg^{-1}, open symbols; and 150 mg/kg^{-1}, closed symbols). Data are expressed relative to pre-injection levels. Values are means ± standard error; $n = 3$ per group). Difference between the groups was significant ($p < 0.05$).

LCBF levels in ACZ-treated rats were significantly elevated above those of untreated-injured rats in a number of important areas, including the pericontusional margin, thalamus, corpus callosum, and internal capsule ($p < 0.05$, Fig. 3C), such that values were not significantly different from sham-control levels. Even within the external capsule and cingulum, LCBF values were trending close to, or above sham values. On average, LCBF values in the ACZ group were 88% and 68% higher in the ipsilateral and contralateral hemispheres, respectively, compared with the untreated-injured group. Contralateral LCBF in untreated-injured rats was not significantly different from sham-control rats as shown by the closeness of values to the 100% sham-injured line (Fig. 3C), and ACZ-treatment resulted in levels that were 50–125% above normal in 9 of 10 structures examined (Fig. 3C; Table 2).

Brain LCMRglc is unaffected by acetazolamide

Next we examined the effect of ACZ administration on LCMRglc values in the same rats assessed for LCBF using dual-probe autoradiography. We found that unlike the effect on LCBF values, acute ACZ resulted in no significant effect on LCMRglc in any brain region examined (Fig. 4A–C). There was a trend towards reduced LCMRglc values throughout most of the brain (Fig. 4C), and this was especially notable in hippocampal regions, where levels are normally elevated in injured-untreated rats in the initial post-injury period (Fig. 4A versus 4B; Table 2). While on average LCMRglc values in the ACZ group were reduced by 15% and 11% in the ipsilateral and contralateral hemisphere, respectively, when compared with the untreated-injured group, variability among individual treated rats resulted in no significant difference within the individual structures when compared with the untreated-injured group (Fig. 4C).

LCMRglc:LCBF ratio is normalized by acetazolamide

By computation of the metabolism:flow ratio of LCMRglc:LCBF from the co-registered, parametric autoradiographic

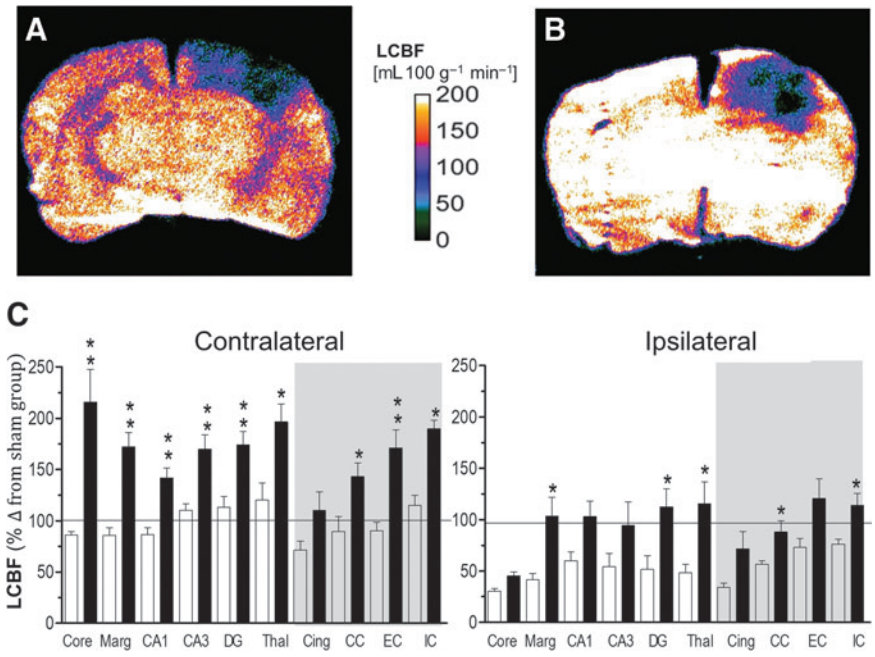

FIG. 3. Representative local cerebral blood flow (LCBF) parametric maps from an injured untreated (**A**) and an acetazolamide (ACZ)-treated rat (**B**) at 3 h after injury, and (**C**) bar graphs of quantified contralateral and ipsilateral LCBF values (as percentages of the corresponding sham control region of interest [ROI] values) in untreated-injured (open bars), and ACZ-treated rats (solid bars), at 3 h post-trauma in grey and white matter (shaded area) brain regions. Administration of ACZ resulted in a global increase in LCBF that was maintained in both grey and white matter regions until 3 h post-injury (**A** versus **B**). LCBF values were significantly increased bilaterally in most regions of the brain compared to untreated, injured rats, such that values were similar to or above those in sham-injured rats (horizontal line). Data are plotted as means ± standard error of the mean; $*p < 0.05$, $**p < 0.01$ corrected for multiple comparisons; Core, contusion core; Marg, pericontusion margin; Cing, cingulum; Thal, thalamus; CC, corpus callosum; EC, external capsule; IC, internal capsule; DG, dentate gyrus). Color image is available online at www.liebertonline.com/neu

datasets, we found that there was a significant uncoupling, or mismatch, between flow and metabolism in untreated rats at 3 h post-injury compared to sham-injured animals. There was a significant rise in this ratio (i.e., metabolism > flow) throughout most structures of the ipsilateral hemisphere, particularly in the pericontusion margin, where it was increased by up to 217% (Fig. 5A–C; Table 2). However, we found that ACZ administration significantly reduced this ratio, mostly through an increase in LCBF, but also due to smaller decreases in LCMRglc. This occurred throughout most of the brain compared to untreated-injured rats ($p < 0.05$), so that values were similar to the sham-injured group; for example, metabolism:flow was reduced by 71% in the pericontusion margin compared to the untreated-injured group ($p < 0.01$). Although there was no effect of ACZ in the contusion core and internal capsule, these regions were not significantly affected by injury compared to sham-injured rats (Figs. 3C and 5C).

Accumulation of β-APP is attenuated by acute improvements in LCBF

We next investigated whether acute ACZ administration to reduce early cerebrovascular dysfunction has a beneficial effect by preventing ongoing axonal injury. We found that the anatomical localization and the morphology of individual β-APP-immunopositive axonal foci in the ACZ-treated groups were similar to those in the untreated-injured group (Fig. 6A). The burden of axonal injury was confined closer to the injury site around the cingulum and corpus callosum, with less damage in more remote structures such as the thalamus. Semi-quantitative assessment of β-APP profiles in frozen sections adjacent to those used for autoradiography at 3 h after ACZ administration revealed no significant differences from the untreated-injured group in all structures apart from the thalamus, where there was a significant reduction ($p < 0.01$; Fig. 6B). However, at 24 h after ACZ, the mean densities of β-APP profiles significantly decreased in the cingulum ($p < 0.001$), the posterior corpus callosum ($p < 0.01$), the contusion margin ($p < 0.01$), and the thalamus ($p < 0.01$), when compared to the untreated-injured group. Apart from the contusion margin, ACZ treatment prevented further axonal injury since there was no significant difference in the mean density of β-APP from 3 to 24 h in any white or grey matter region examined ($p < 0.05$).

Acute increases in LCBF may not protect all injured axonal populations equally

In a separate cohort of rats at 24 h after injury, we examined whether the positive effects of ACZ treatment extended to neurofilament-compacted, RMO14-positive, injured axons, as well as those β-APP-positive axons that were at risk of injury due to dysfunction in fast axonal transport. One ACZ-treated injured rat and two vehicle-treated rats were not analyzed cohort due to gross structural damage to the corpus callosum that would have introduced bias into the stereologic analysis.

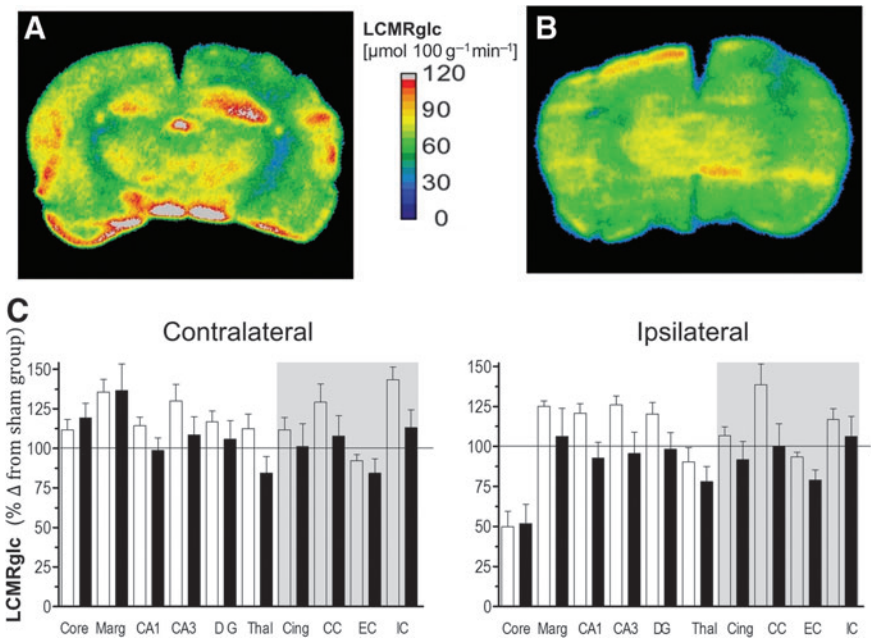

FIG. 4. Representative local cerebral metabolic rate for glucose (LCMRglc) parametric maps from an injured, untreated (**A**) and acetazolamide (ACZ)-treated rat (**B**) at 3 h after injury, and (**C**) bar graphs of quantified contralateral and ipsilateral LCMRglc values (as percentages of the corresponding sham control region-of-interest [ROI] values) in untreated-injured (open bars) and ACZ-treated rats (solid bars) at 3 h post-trauma in grey and white matter (shaded area) brain regions. Despite the observation that injury-induced hyperglycolysis (the high LCMRglc values in **A**) was often normalized by ACZ (**A** versus **B**), wide variability between animals (e.g., ipsilateral and marginal zone, **C**) resulted in the finding that there was no significant effect of ACZ treatment on LCMRglc in any brain region measured. Data are plotted as means ± standard error of the mean; the horizontal line represents sham-injured values (Core, contusion core; Marg, pericontusion margin; Cing, cingulum; Thal, thalamus; CC, corpus callosum; EC, external capsule; IC, internal capsule; DG, dentate gyrus). Color image is available online at www.liebertonline.com/neu

Despite this reduction in group sizes ($n = 7$ and 4, in ACZ and vehicle-treated injured groups, respectively), the statistical power calculated by group comparisons was greater than 80%, so any differences most likely would be detectable. Consistent with previously reported data, we found that there was no overlap between RMO14- and β-APP-positive profiles, so they can be considered as two distinct populations of injured axons (Fig. 7B). Stereological analysis of perfusion-fixed sections of the cingulum and corpus callosum underlying the injury core (Fig. 7A) revealed a significant reduction in the number of β-APP-positive profiles in the ACZ-treated group compared to vehicle-treated animals (Fig. 7C and D, and E and F; $p < 0.01$). This is in agreement with the less robust, but more global analysis of reduced β-APP profiles in ACZ-treated injured rats, performed in frozen sections adjacent to the autoradiographic sections, within ROIs that exhibited LCMRglc:LCBF ratios similar to sham-control animals (Fig. 6). However, we also found that early intervention did not robustly normalize microstructural axon damage as indicated by RMO14 staining. Although the number of RMO14-positive axons, an indicator of neurofilament compaction, was reduced in the ACZ-treated group compared to vehicle-treated animals, this difference did not reach significance. Finally, we determined whether ACZ treatment prevented expansion of the lesion. Estimates of ipsilateral cortical grey and white matter volume loss as a percentage of the contralateral cortex of the 5 sections used for assessment of axon pathology showed that there was no difference (9.1 ± 2.3% and 9.8 ± 2.5% in the saline-treated and ACZ-treated groups), indicating that at least at 24 h after injury, axonal sparing did not occur commensurate with the reduction in cortical atrophy.

Discussion

In this study, we have shown that the administration of ACZ immediately following CCI injury results in a significant increase in post-traumatic LCBF, but no significant change in LCMRglc. The net result is to diminish the pronounced uncoupling (i.e., when metabolism > blood flow) that otherwise occurs during the acute stage of injury. In the same brain regions that acutely exhibited more normal levels of flow/metabolism as a consequence of the ACZ intervention, the development of impaired axonal transport and delayed axotomy between 3 and 24 h was attenuated, as indicated by a significant reduction in β-APP immunoreactivity at 24 h when compared to vehicle-treated, injured rats. Although this intervention did result in a trend toward less neurofilament compaction in an entirely separate population of injured axons, this was variable and did not reach significance.

Reduction of flow/metabolism uncoupling acutely prevents further injury in β-APP axons

The present results extend our previous investigations obtained in rats studied at 3 h after the same CCI injury (Chen et al., 2004), for which moderate hypoperfusion in the

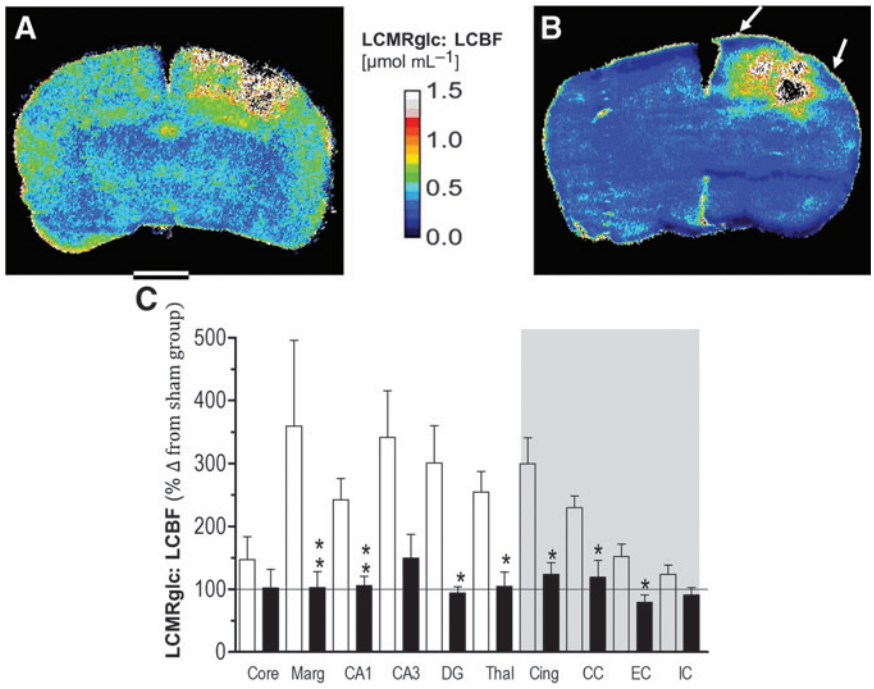

FIG. 5. Representative parametric maps from an injured, untreated (**A**) and acetazolamide (ACZ)-treated rat (**B**) at 3 h after trauma for the calculated ratio of LCMRglc: LCBF. The ratio between flow and metabolism was decreased globally by ACZ (**B**), and this extended to the pericontusion margin (arrows). (**C**) Bar graph demonstrating ipsilateral LCMRglc:LCBF ratio values (as percentages of the corresponding sham-control region-of-interest [ROI] data) in untreated-injured (open bars) and ACZ-treated rats (solid bars) in grey and white matter (shaded area) brain regions. ACZ significantly reduced the ratios in most regions of the ipsilateral hemisphere, including the pericontusion margin. Data are plotted as means ± standard error of the mean; the horizontal line represents sham-injured values. (Core, contusion core; Marg, pericontusion margin; Cing, cingulum; Thal, thalamus; CC, corpus callosum; EC, external capsule; IC, internal capsule; DG, dentate gyrus; LCMRglc:LCBF, local cerebral metabolic rate for glucose:local cerebral blood flow ratio). Color image is available online at www.liebertonline.com/neu

ipsilateral hemispheric coexisted with a paradoxically normal or increased metabolic rate for glucose, resulting in regions of marked metabolism > flow dissociation (i.e., uncoupling). This previous work demonstrated that early uncoupling was a regionally-specific process affecting predominantly the contusion margin, ipsilateral hippocampus, thalamus, cingulum, and corpus callosum, and that in white matter regions the degree of uncoupling was positively associated with the development of axonal injury. Although the degree of LCBF reduction did not reach levels typically associated with energy failure (Hossmann, 1994) it occurred during a period when the brain was experiencing an increased energy demand in the same areas, so that the metabolic stress that develops may be regarded as an important factor contributing to the development of axonal injury. In the present study, ACZ administration markedly ameliorated the early metabolic stress attributable to post-injury metabolism-blood flow uncoupling, and prevented further injury among the β-APP-stained population of injured axons.

Although not directly related to the issue of axonal injury, work in other laboratories supports our findings that normalization of early flow-metabolism uncoupling might contribute to neuroprotection. A significant reduction in contusion size and/or improvement in neurological function after experimental TBI was attained by reducing the initial uncoupling, or attenuating the CBF reduction, by early administration of either high-dose human albumin therapy (Belayev et al., 1999; Ginsberg et al., 2001), a nitrone radical scavenger (Marklund et al., 2002), a low dose of ethanol (Kelly et al., 1997, 2000), or L-arginine (Cherian et al., 1999), or an oxygen radical scavenger (Hamm et al., 1996; Muir et al., 1995). However, in contrast to these studies, post-traumatic hypothermia resulted in a near doubling of the LCMRglc:LCBF ratio at 6 h after fluid percussion injury (Zhao et al., 1999), a paradoxical decrease in neurofilament-stained axons at 24 h after rat contusion injury (Marion and White, 1996), and improved sensorimotor and cognitive behavior at later time points (Bramlett et al., 1995). Taken together, these observations suggest that early flow-metabolism uncoupling contributes significantly to the injury process, while uncoupling at more chronic time points may not endanger cerebral recovery. It will be important to define the extent of this critical period during which the maintenance of flow-metabolism coupling after injury is absolutely required in order to prevent further axonal damage, in different species including humans.

Mechanism of action of improved flow-metabolism

The mechanism whereby normalizing flow-metabolism uncoupling provides neuroprotection is uncertain. It is likely that early reductions in the metabolic stress attributed to reducing post-traumatic uncoupling helps to prevent the onset of axolemmal permeability change, calcium influx, and

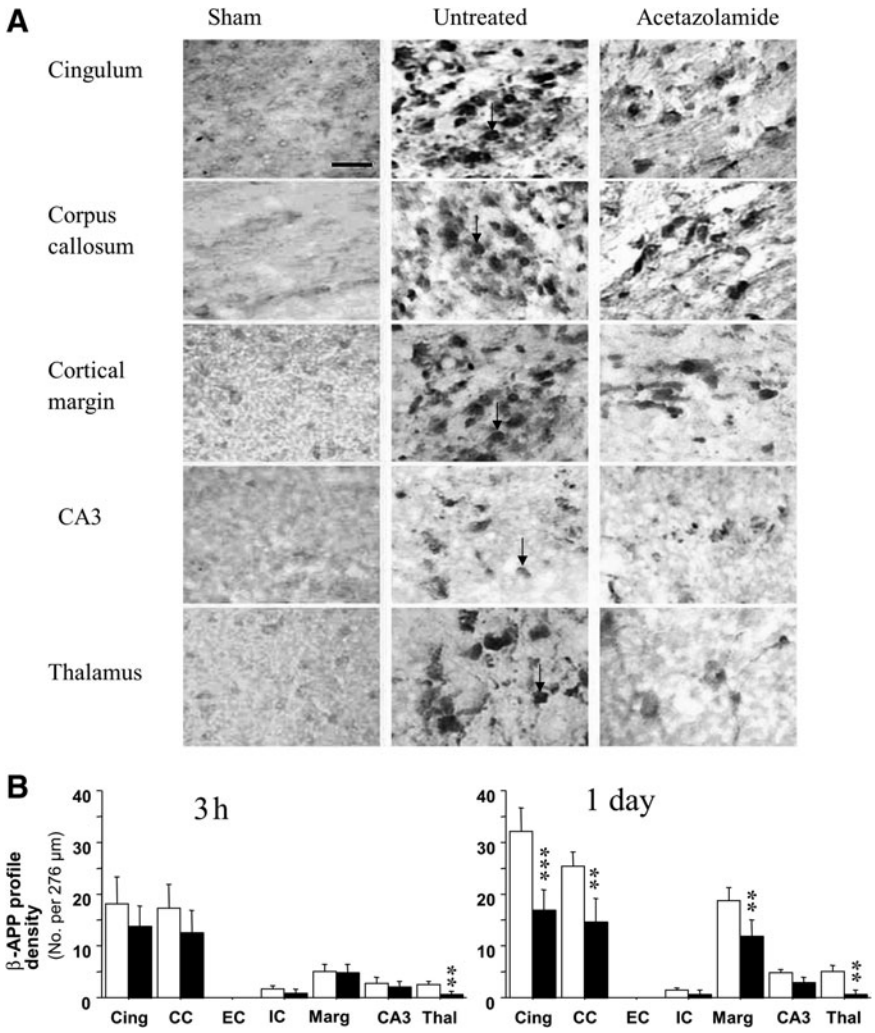

FIG. 6. (**A**) High-power views showing β-APP immunoreactivity in different ipsilateral brain regions at 1 day after injury in ACZ-treated animals compared with sham-control and untreated-injured animals. Note that the number of damaged immunoreactive axons (arrows) was significantly reduced in ACZ-treated animals compared with untreated-injured animals (scale bar = 20 μm). (**B**) Bar graph of the mean densities of immunopositive profiles displaying β-APP immunoreactivity in ACZ-treated (solid bars) and untreated-injured rats (open bars) at 3 and 24 h after trauma. There was a significant decrease in the number of β-APP-immunopositive damaged axons in the cingulum, corpus callosum, pericontusion margin, and thalamus in the ACZ group at 24 h. Data are plotted as means ± standard error of the mean (Marg, pericontusion margin; Cing, cingulum; Thal, thalamus; CC, corpus callosum; EC, external capsule; IC, internal capsule; ACZ, acetazolamide; β-APP, β-amyloid precursor protein).

mitochondrial damage, all of which are considered to play pivotal roles in initiating progressive axonal changes (Maxwell et al., 1997). It is conceivable that the mechanism through which ACZ improves axonal outcome is by a blood flow-mediated improvement in both oxygen availability (through both substrate delivery and as a function of ACZ-induced, pH-mediated alterations in the hemoglobin dissociation curve), and a reduction in the concentration of excitotoxic agonists, such as glutamate and potassium ions, similar to that observed after ischemia-reperfusion (Harris et al., 2000). This dual effect would reduce the energy deficit by decreasing glycolytic metabolism in favor of more efficient energy production via oxidative metabolism, while also relieving energy demand by decreasing excitotoxic-induced membrane depolarization. Within the current paradigm, the net effect might be measured as a reduction in LCMRglc, and although not significant, the present results do demonstrate a global trend towards a reduction in LCMRglc with ACZ treatment. If values for cerebral metabolic rate of oxygen use were available, it might be reflected in an improvement in the metabolic ratio, the molar ratio of oxygen to glucose use. In support of this, hyperbaric oxygen therapy has been shown to prevent ischemia-induced cell death (Yang et al., 2001), presumably by either improvement of oxidative metabolism by supplying mitochondria with more oxygen, or by oxygen-enhanced reperfusion. Hyperbaric oxygen therapy in brain-injured patients had similar cerebrovascular effects to those discussed above—acutely increased CBF and cerebral metabolic rate of oxygen ($CMRO_2$) and, together with a reduced CSF lactate concentration, this indicates enhanced oxidative metabolism (Rockswold et al., 2001). However, most importantly, neurological outcome was not addressed in that study, which

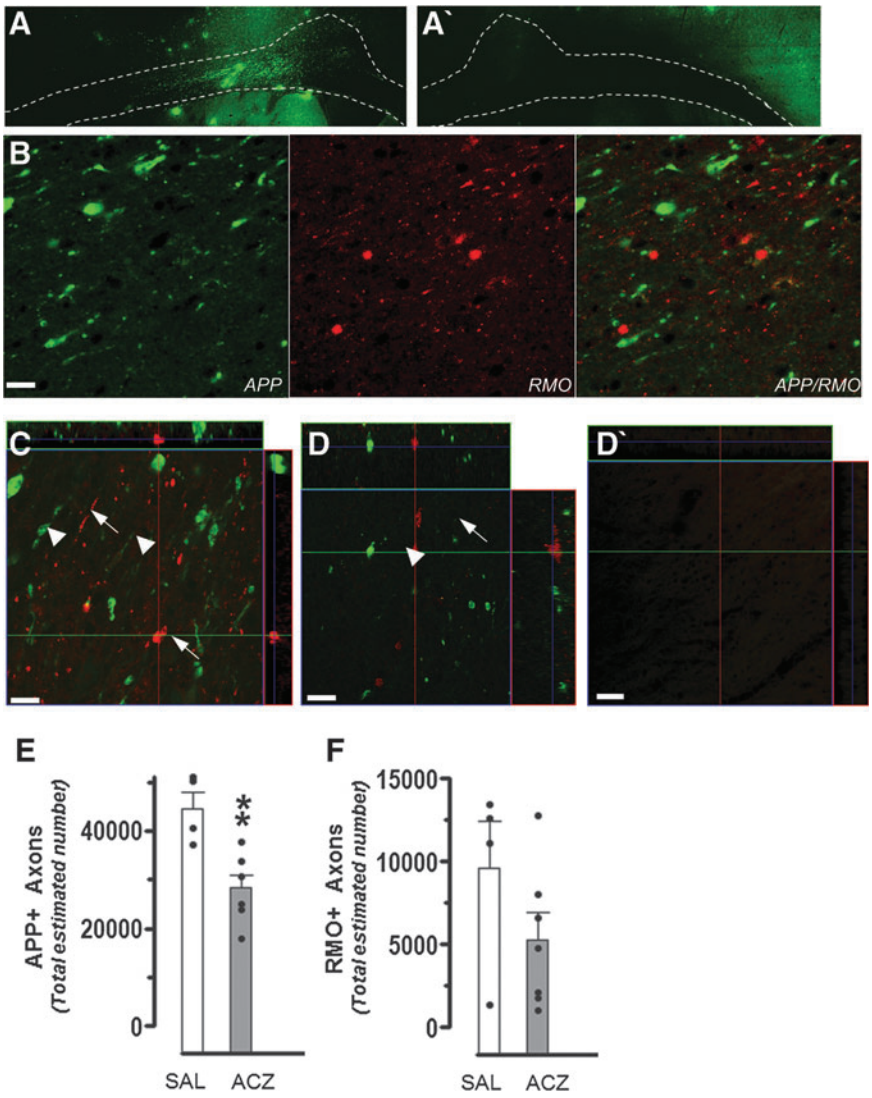

FIG. 7. (**A**) Representative coronal montages of β-APP immunostaining within the corpus callosum and cingulum under the impact zone ipsilaterally at 24 h in a vehicle-treated rat demonstrating the contoured region in which the stereological analyses were performed. (**A'**) A montage image of the corresponding contralateral hemisphere montage of the same vehicle-injured rat showing an absence of β-APP immunostaining in the white matter (contoured area). (**B**) Representative high-power images showing positive staining for β-APP (green), and RMO14 (red) in the corpus callosum of a vehicle-treated, injured rat at 24 h. Consistent with previously reported results, there is no overlap between staining, which suggests that impaired axonal transport and neurofilament compaction may be occurring in either different populations of axons, or in different parts of the same axon. (**C** and **D**) Representative high-power confocal z-stack images of the corpus callosum underlying the injury core immunostained for β-APP (green) and RMO14 (red) from (**C**) a vehicle-treated injured rat, and (**D**) an ACZ-treated injured rat. Bulb-like swelling and punctate profiles (arrowheads) are associated with β-APP-positive axons. RMO14-positive axons are thin and elongated or display vacuolization (arrows). Note the overall decrease in the amount of positive staining for both β-APP and RMO14 in ACZ compared to vehicle animals (scale bars = 10 μm). (**D'**) A representative β-APP/RMO14 image of the contralateral corpus callosum of a vehicle-injured rat acquired with the same acquisition parameters (gain/offset) as the other high-powered images. The absence of RMO14-positive profiles in this region indicates that axonal injury is specific to the ipsilateral callosum at this post-injury time point. Bar graphs of the stereologically-estimated number of ipsilateral (**E**) β-APP, and (**F**) RMO14-positive axons in saline vehicle-treated (SAL, open bars), and ACZ-treated (ACZ, solid bars) at 24 h post-injury as determined by stereology. Data are plotted as means ± standard error of the mean, and individual data from each rat are over-plotted (closed dots; $^{**}p < 0.01$; ACZ, acetazolamide; β-APP, β-amyloid precursor protein). Color image is available online at www.liebertonline.com/neu

largely precludes drawing any conclusions about the efficacy of any therapeutic benefit.

There is evidence to suggest that the brain is able to utilize alternative metabolic substrates under conditions of energy crisis, for example, lactate and pyruvate (Chen et al., 2000; Moro and Sutton, 2010; Schurr et al., 1999). A therapy aimed at increasing blood flow to the contused brain would most likely increase the availability of these substrates to tissues in metabolic crisis, which could increase energy production through oxidative metabolism and thus reduce the dependence on glycolysis, which is already increased in the acute stages of injury (Yoshino et al., 1991). The axolemma can

continue to leak for several hours after injury, and this is likely to be associated with continued calcium influx, calpain-mediated spectrin proteolysis, and subsequent modification of the axolemma, contributing to an exacerbated axolemmal leak (Povlishock and Pettus, 1996). Perhaps by maintaining flow-metabolism coupling in the first few hours after trauma, this damaging cascade of reactions is blunted, allowing the axolemma to reseal and thereby restoring axon integrity, and quite possibly neuronal function. New evidence suggests that after mild brain injury without contusion, diffuse axon injury as indicated by β-APP immunoreactivity results in neuronal atrophy and not cell death (Greer et al., 2011). It will therefore be of interest in future studies to determine whether early intervention to reduce flow/metabolism uncoupling can prevent this type of pathology, and whether functional benefits result.

Another possibility to explain the improvements in outcome among β-APP-stained axons in this study is that there was a direct neuroprotective effect of ACZ. However, to our knowledge, the main effect of ACZ is to inhibit carbonic anhydrase, thus resulting in CO_2 retention and concomitant pH reduction (Bickler et al., 1988). There is no evidence that this substance exerts any direct cytoprotective effect, and our data showing no reductions in tissue atrophy in the ACZ group tends to supports this. Furthermore, the abundance of evidence that demonstrates normalized uncoupling through other treatments leading to good outcomes (Belayev et al., 1999; Ginsberg et al., 2001; Kelly et al., 2000), tend to support the idea that further injury is prevented by reducing local metabolic stress through a cerebrovascular effect.

Restoration of flow/metabolism coupling may not protect different populations of injured axons equally

Treatment to normalize uncoupling did not prevent some axonal injury β-APP from developing at 3 h, despite prompt treatment. While intravascular rather than intraperitoneal administration of ACZ might have prevented this to some extent by producing an immediate rise in blood flow, it is likely that at least some axons are irretrievably damaged after the initial insult and are not amenable to any type of treatment. Manipulation of LCBF after brain injury can lead to an intracerebral "steal" phenomenon, a paradoxical decrease in flow in susceptible areas (Harris et al., 2001), and this could exacerbate axonal injury in the current model. However, there was a relatively global effect of ACZ on LCBF and the LCMRglc:LCBF ratio in the current data, with no negative effects in the contusion core or margin, regions that may be particularly vulnerable to LCBF steal. Of paramount importance for any potential therapy is the ability to enhance functional outcome so that an experiment designed to assess motor recovery using the same treatment protocol merits consideration in future studies.

The finding that despite normal flow metabolism, the number of neurofilament-compacted neurons and the degree of tissue atrophy was not significantly ameliorated 24 h later, suggests that this intervention alone might not be sufficient to prevent injury among all populations of injured axons. This could well relate to the severity of the axon injury; axotomy can be rapid (Kelly et al., 2006), so that later measurements of tissue atrophy and neurofilament compaction might well show a beneficial effect of intervention. The absence of a statistically significant effect of intervention among this population of axons might also relate to their myelination status, because although findings similar to the current study have been reported using the calcineurin inhibitor FK506 after impact acceleration injury (Marmarou and Povlishock, 2006), this was later shown to be most efficacious in unmyelinated axons (Reeves et al., 2007). Blocking the mitochondrial pore using cyclosporin A after injury was shown to significantly attenuate neurofilament compaction, possibly by enabling the restoration of ionic and metabolic homeostasis (Buki et al., 1999a). This underscores the idea that a combination of therapies are required to blunt the multifaceted nature of axonal pathology after TBI. Despite the absence of a significant effect on both populations of axons, it should be noted that the relationship between β-APP- and RMO14-immunoreactive markers of axonal pathology after TBI has not been entirely resolved. For example, the degree of phosphorylation (i.e., injury-induced dephosphorylation) of neurofilament side arms may greatly influence the effect on axonal transport (Nixon et al., 1994a,1994b), and hence the accumulation of β-APP protein; yet the two pathologies remain in different injured axon populations after TBI (Stone et al., 2004). This might indicate that the antibodies are insensitive to less severe axonal injury, and indeed, it has been suggested that cytoskeletal compaction of axons is spread over much greater distances when assessed by silver staining (Gallyas et al., 2002) compared to other studies using RMO14 antibody.

In summary, this study provides quantitative evidence that augmentation of LCBF to prevent uncoupling early after experimental trauma is neuroprotective by preventing secondary injury in at least one population of injured axons. Our previous study demonstrated that the development of secondary TAI was likely to be related to the degree of the initial LCBF reduction and flow-metabolism uncoupling, and we now provide evidence that post-injury circulatory and metabolic dysfunctions contribute to delayed axonal injury. These findings demonstrate the importance of maintaining flow-metabolism coupling early after injury as one therapeutic target for blunting the secondary cascade of reactions that lead to axonal injury.

Acknowledgments

This work was supported by the Medical Research Council of the United Kingdom, National Institutes of Health/National Institute of Neurological Disorders and Stroke award no. NS055910 and the UCLA Brain Injury Research Center. The Overseas Research Council and Merck Sharp & Dohme funded S.F.C. and N.G.H., respectively. We would also like to thank Ms. Marcia Nogueira for her assistance with the experiments.

Author Disclosure Statement

No competing financial interests exist.

References

Adams, J.H., Doyle, D., Ford, I., Gennarelli, T.A, Graham, D.I, and McLellan, D.R. (1989). Diffuse axonal injury in head injury: definition, diagnosis and grading. Histopathology 15, 49–59.

Belayev, L., Alonso, O.F., Huh, P.W, Zhao, W., Busto, R., and Ginsberg, M.D. (1999). Post treatment with high-dose albumin reduces histopathological damage and improves neurological

deficit following fluid percussion brain injury in rats. J. Neurotrauma 16, 445–453.

Benjamini, Y., and Hochberg, Y. (1995). Controlling the false discovery rate: a practical and powerful approach to multiple testing. J. R. Statist. Soc. 57, 289–300.

Bergsneider, M., Hovda, D.A., Shalmon, E., Kelly, D.F., Vespa, P.M., Martin, N.A., Phelps, M.E., McArthur, D.L., Caron, M.J., Kraus, J.F., and Becker, D.P. (1997). Cerebral hyperglycolysis following severe traumatic brain injury in humans: a positron emission tomography study. J. Neurosurg. 86, 241–251.

Bickler, P.E., Litt, L., Banville, D.L., and Severinghaus, J.W. (1988). Effects of acetazolamide on cerebral acid-base balance. J. Appl. Physiol. 65, 422–427.

Bouma, G.J., and Muizelaar, J.P. (1992). Cerebral blood flow, cerebral blood volume, and cerebrovascular reactivity after severe head injury. J. Neurotrauma 9(Suppl. 1), S333–S348.

Bouma, G.J., Muizelaar, J.P., Choi, S.C., Newlon, P.G., and Young, H.F. (1991). Cerebral circulation and metabolism after severe traumatic brain injury: the elusive role of ischemia. J. Neurosurg. 75, 685–693.

Bramlett, H.M., Green, E.J., Dietrich, W.D., Busto, R., Globus, M.Y., and Ginsberg, M.D. (1995). Posttraumatic brain hypothermia provides protection from sensorimotor and cognitive behavioral deficits. J. Neurotrauma 12, 289–298.

Bryan, R.M., Jr., Cherian, L., and Robertson, C. (1995). Regional cerebral blood flow after controlled cortical impact injury in rats. Anesth. Analg. 80, 687–695.

Buki, A., Okonkwo, D.O., and Povlishock, J.T. (1999a). Postinjury cyclosporin A administration limits axonal damage and disconnection in traumatic brain injury. J. Neurotrauma 16, 511–521.

Buki, A., Okonkwo, D.O., Wang, K.K., and Povlishock, J.T. (2000). Cytochrome c release and caspase activation in traumatic axonal injury. J. Neurosci. 20, 2825–2834.

Buki, A., Siman, R., Trojanowski, J.Q., and Povlishock, J.T. (1999b). The role of calpain-mediated spectrin proteolysis in traumatically induced axonal injury. J. Neuropathol. Exp. Neurol. 58, 365–375.

Chen, S., Pickard, J.D., and Harris, N.G. (2003). Time-course of cellular pathology after controlled cortical impact injury. Exp. Neurol. 182, 87–102.

Chen, S., Richards, H.K., Smielewski, P., Johnstrom, P., Salvador, R., Pickard, J.D., and Harris, N.G. (2004). Relationship between flow-metabolism uncoupling and evolving axonal injury after experimental traumatic brain injury. J. Cereb. Blood Flow Metab. 24, 1025–1036.

Chen, T., Qian, Y.Z., Rice, A., Zhu, J.P., Di, X., and Bullock, R. (2000). Brain lactate uptake increases at the site of impact after traumatic brain injury. Brain Res. 861, 281–287.

Cherian, L., Chacko, G., Goodman, J.C., and Robertson, C.S. (1999). Cerebral hemodynamic effects of phenylephrine and L-arginine after cortical impact injury. Crit. Care Med. 27, 2512–2517.

Christman, C.W., Grady, M.S., Walker, S.A., Holloway, K.L., and Povlishock, J.T. (1994). Ultrastructural studies of diffuse axonal injury in humans. J. Neurotrauma 11, 173–186.

Coles, J.P., Minhas, P.S., Fryer, T.D., Smielewski, P., Aigbirihio, F., Donovan, T., Downey, S.P., Williams, G., Chatfield, D., Matthews, J.C., Gupta, A.K., Carpenter, T.A., Clark, J.C., Pickard, J.D., and Menon, D.K. (2002). Effect of hyperventilation on cerebral blood flow in traumatic head injury: clinical relevance and monitoring correlates. Crit. Care Med. 30, 1950–1959.

Forbes, M.L., Hendrich, K.S., Kochanek, P.M., Williams, D.S., Schiding, J.K., Wisniewski, S.R., Kelsey, S.F., DeKosky, S.T., Graham, S.H., Marion, D.W., and Ho, C. (1997). Assessment of cerebral blood flow and CO_2 reactivity after controlled cortical impact by perfusion magnetic resonance imaging using arterial spin-labeling in rats. J. Cereb. Blood Flow Metab. 17, 865–874.

Gallyas, F., Pat, J., Farkas, O., Dóczi, T. (2006). The fate of axons subjected to traumatic ultrastructural (neurofilament) compaction: an electron-microscopic study. Acta neuropathologica 111, 229–237.

Gentleman, S.M., Nash, M.J., Sweeting, C.J., Graham, D.I., and Roberts, G.W. (1993). Beta-amyloid precursor protein (beta APP) as a marker for axonal injury after head injury. Neurosci. Lett. 160, 139–144.

Ginsberg, M.D., Zhao, W., Belayev, L., Alonso, O.F., Liu, Y., Loor, J.Y., and Busto, R. (2001). Diminution of metabolism/blood flow uncoupling following traumatic brain injury in rats in response to high-dose human albumin treatment. J. Neurosurg. 94, 499–509.

Greer, J.E., McGinn, M.J., and Povlishock, J.T. (2011). Diffuse traumatic axonal injury in the mouse induces atrophy, c-Jun activation, and axonal outgrowth in the axotomized neuronal population. J. Neurosci. 30, 5089–5105.

Grady, M.S., McLaughlin, M.R., Christman, C.W., Valadka, A.B., Fligner, C.L., and Povlishock, J.T. (1993). The use of antibodies targeted against the neurofilament subunits for the detection of diffuse axonal injury in humans. J. Neuropathol. Exp. Neurol. 52, 143–152.

Hamm, R.J., Temple, M.D., Pike, B.R., and Ellis, E.F. (1996). The effect of postinjury administration of polyethylene glycol-conjugated superoxide dismutase (pegorgotein, Dismutec) or lidocaine on behavioral function following fluid-percussion brain injury in rats. J. Neurotrauma 13, 325–332.

Harris, N.G., Lythgoe, M.F., Thomas, D.L., and Williams, S.R. (2001). Cerebrovascular reactivity following focal brain ischemia in the rat: a functional magnetic resonance imaging study. Neuroimage 13, 339–350.

Harris, N.G., Hovda, D.A., and Sutton, R.L. (2009). Acute deficits in transcallosal connectivity endure chronically after experimental brain injury in the rat: a DTI tractography study. J. Neurotrauma 26, A37 (Abstract).

Harris, N.G., Zilkha, E., Houseman, J., Symms, M.R., Obrenovitch, T.P., and Williams, S.R. (2000). The relationship between the apparent diffusion coefficient measured by magnetic resonance imaging, anoxic depolarization, and glutamate efflux during experimental cerebral ischemia. J. Cereb. Blood Flow Metab. 20, 28–36.

Hossmann, K.A. (1994). Viability thresholds and the penumbra of focal ischemia. Ann. Neurol. 36, 557–565.

Ingvar, M., Eriksson, L., Rogers, G.A., Stone-Elander, S., and Widen, L. (1991). Rapid feasibility studies of tracers for positron emission tomography: high-resolution PET in small animals with kinetic analysis. J. Cereb. Blood Flow Metab. 11, 926–931.

Kelley, B.J., Farkas, O., Lifshitz, J, and Povlishock, J.T. (2006). Traumatic axonal injury in the perisomatic domain triggers ultrarapid secondary axotomy and Wallerian degeneration. Exp. Neurol. 198, 350–360.

Kelly, D.F., Lee, S.M., Pinanong, P.A., and Hovda, D.A. (1997). Paradoxical effects of acute ethanolism in experimental brain injury. J .Neurosurg. 86, 876–882.

Kelly, D.F., Kozlowski, D.A., Haddad, E., Echiverri, A., Hovda, D.A., and Lee, S.M. (2000). Ethanol reduces metabolic

uncoupling following experimental head injury. J. Neurotrauma 17, 261–272.

Kochanek, P.M., Marion, D.W., Zhang, W., Schiding, J.K., White, M., Palmer, A.M., Clark, R.S., O'Malley, M.E., Styren, S.D., and Ho, C. (1995). Severe controlled cortical impact in rats: assessment of cerebral edema, blood flow, and contusion volume. J. Neurotrauma 12, 1015–1025.

Lear, J.L., and Ackermann, R.F. (1989). Regional comparison of the lumped constants of deoxyglucose and fluorodeoxyglucose. Metab. Brain Dis. 4, 95–104.

Marion, D.W., Darby, J., and Yonas, H. (1991). Acute regional cerebral blood flow changes caused by severe head injuries. J. Neurosurg. 74, 407–414.

Marion, D.W., and White, M.J. (1996). Treatment of experimental brain injury with moderate hypothermia and 21-aminosteroids. J. Neurotrauma 13, 139–147.

Marklund, N., Sihver, S., Langstrom, B., Bergstrom, M., and Hillered, L. (2002). Effect of traumatic brain injury and nitrone radical scavengers on relative changes in regional cerebral blood flow and glucose uptake in rats. J. Neurotrauma 19, 1139–1153.

Marmarou, C.R., and Povlishock, J.T. (2006). Administration of the immunophilin ligand FK506 differentially attenuates neurofilament compaction and impaired axonal transport in injured axons following diffuse traumatic brain injury. Exp. Neurol. 197, 353–362. Epub 2005 Nov 17.

Marmarou, C.R., Walker, S.A., Lewis, C.L., and Povlishock, J.T. (2005). quantitative analysis of the relationship between intra-axonal neurofilament compaction and impaired axonal transport following diffuse traumatic brain injury. J. Neurotrauma 10, 1066–1080.

Martin, N.A., Patwardhan, R.V., Alexander, M.J., Africk, C.Z., Lee, J.H., Shalmon, E., Hovda, D.A., and Becker, D.P. (1997). Characterization of cerebral hemodynamic phases following severe head trauma: hypoperfusion, hyperemia, and vasospasm. J. Neurosurg. 87, 9–19.

Maxwell, W.L., Kosanlavit, R., McCreath, B.J., Reid, O., and Graham, D.I. (1999). Freeze-fracture and cytochemical evidence for structural and functional alteration in the axolemma and myelin sheath of adult guinea pig optic nerve fibers after stretch injury. J. Neurotrauma 16, 273–284.

Maxwell, W.L., McCreath, B.J., Graham, D.I., and Gennarelli, T.A. (1995). Cytochemical evidence for redistribution of membrane pump calcium-ATPase and ecto-Ca-ATPase activity, and calcium influx in myelinated nerve fibres of the optic nerve after stretch injury. J. Neurocytol. 24, 925–942.

Maxwell, W.L., Povlishock, J.T., and Graham, D.L. (1997). A mechanistic analysis of nondisruptive axonal injury: a review. J. Neurotrauma 14, 419–440.

Maxwell, W.L., Watt, C., Graham, D.I., and Gennarelli, T.A. (1993). Ultrastructural evidence of axonal shearing as a result of lateral acceleration of the head in non-human primates. Acta Neuropathol. (Berl.) 86, 136–144.

Moro, N., and Sutton, R.L. (2010). Beneficial effects of sodium or ethyl pyruvate after traumatic brain injury in the rat. Exp. Neurol. 225, 391–401.

Muir, J.K., Tynan, M., Caldwell, R., and Ellis, E.F. (1995). Superoxide dismutase improves posttraumatic cortical blood flow in rats. J. Neurotrauma 12, 179–188.

Nixon, R.A., Lewis, S.E., Mercken, M., and Sihag, R.K. (1994b). [32P]orthophosphate and [35S]methionine label separate pools of neurofilaments with markedly different axonal transport kinetics in mouse retinal ganglion cells in vivo. Neurochem. Res. 19, 1445–1453.

Nixon, R.A., Paskevich, P.A., Sihag, R.K., and Thayer, C.Y. (1994a). Phosphorylation on carboxyl terminus domains of neurofilament proteins in retinal ganglion cell neurons in vivo: influences on regional neurofilament accumulation, interneurofilament spacing, and axon caliber. J. Cell Biol. 126, 1031–1046.

Okonkwo, D.O., Pettus, E.H., Moroi, J., and Povlishock, J.T. (1998). Alteration of the neurofilament sidearm and its relation to neurofilament compaction occurring with traumatic axonal injury. Brain Res. 784, 1–6.

Paxinos, G., and Watson, C. (1997). *The Rat Brain in Stereotaxic Coordinates*, 3rd ed. Academic Press.

Pettus, E.H., and Povlishock, J.T. (1996). Characterization of a distinct set of intra-axonal ultrastructural changes associated with traumatically induced alteration in axolemmal permeability. Brain Res. 722, 1–11.

Povlishock, J.T., and Pettus, E.H. (1996). Traumatically induced axonal damage: evidence for enduring changes in axolemmal permeability with associated cytoskeletal change. Acta Neurochir. Suppl. (Wien.) 66, 81–86.

Reeves, T.M., Phillips, L.L., Lee, N.N., and Povlishock, J.T. (2007). Preferential neuroprotective effect of tacrolimus (FK506) on unmyelinated axons following traumatic brain injury. Brain Res. 1154, 225–236.

Richards, H.K., Simac, S., Piechnik, S., and Pickard, J.D. (2001). Uncoupling of cerebral blood flow and metabolism after cerebral contusion in the rat. J. Cereb. Blood Flow Metab. 21, 779–781.

Robertson, C.S., Contant, C.F., Gokaslan, Z.L., Narayan, R.K., and Grossman, R.G. (1992). Cerebral blood flow, arteriovenous oxygen difference, and outcome in head injured patients. J. Neurol. Neurosurg. Psychiatry 55:, 594–603.

Rockswold, S.B., Rockswold, G.L., Vargo, J.M., Erickson, C.A., Sutton, R.L., Bergman, T.A., and Biros, M.H. (2001). Effects of hyperbaric oxygen therapy on cerebral metabolism and intracranial pressure in severely brain injured patients. J. Neurosurg. 94, 403–411.

Saatman, K.E., Abai, B., Grosvenor, A., Vorwerk, C.K., Smith, D.H., and Meaney, D.F. (2003). Traumatic axonal injury results in biphasic calpain activation and retrograde transport impairment in mice. J. Cereb. Blood Flow Metab. 23, 34–42.

Saatman, K.E., Bozyczko-Coyne, D., Marcy, V., Siman, R., and McIntosh, T.K. (1996). Prolonged calpain-mediated spectrin breakdown occurs regionally following experimental brain injury in the rat. J. Neuropathol. Exp. Neurol. 55, 850–860.

Schurr, A., Miller, J.J., Payne, R.S., and Rigor, B.M. (1999). An increase in lactate output by brain tissue serves to meet the energy needs of glutamate-activated neurons. J. Neurosci. 19, 34–39.

Singleton, R.H., Zhu, J., Stone, J.R., and Povlishock, J.T. (2002). Traumatically induced axotomy adjacent to the soma does not result in acute neuronal death. J. Neurosci. 22, 791–802.

Stone, J.R, Okonkwo, D.O., Dialo, A.O., Rubin, D.G., Mutlu, L.K., Povlishock, J.T., and Helm, G.A. (2004). Impaired axonal transport and altered axolemmal permeability occur in distinct populations of damaged axons following traumatic brain injury. Exp. Neurol. 190, 59–69.

Stone, J.R., Singleton, R.H., and Povlishock, J.T. (2000). Antibodies to the C-terminus of the beta-amyloid precursor protein (APP): a site specific marker for the detection of traumatic axonal injury. Brain Res. 871, 288–302.

Sunami, K., Nakamura, T., Ozawa, Y., Kubota, M., Namba, H., and Yamaura, A. (1989). Hypermetabolic state following

experimental head injury. Neurosurg. Rev. 12(Suppl. 1), 400–411.

Sutton, R.L., Hovda, D.A., Adelson, P.D., Benzel, E.C., and Becker, D.P. (1994). Metabolic changes following cortical contusion: relationships to edema and morphological changes. Acta Neurochir. Suppl. (Wien.) 60, 446–448.

Yamakami, I., and McIntosh, T.K. (1991). Alterations in regional cerebral blood flow following brain injury in the rat. J. Cereb. Blood Flow Metab. 11, 655–660.

Yang, J.T., Chang, C.N., Lee, T.H., Lin, T.N., Hsu, J.C., Hsu, Y.H., and Wu, J.H. (2001). Hyperbaric oxygen treatment decreases post-ischemic neurotrophin-3 mRNA down-regulation in the rat hippocampus. Neuroreport 12, 3589–3592.

Yoshino, A., Hovda, D.A., Kawamata, T., Katayama, Y., and Becker, D.P. (1991). Dynamic changes in local cerebral glucose utilization following cerebral conclusion in rats: evidence of a hyper- and subsequent hypometabolic state. Brain Res. 561, 106–119.

Zhao, W., Alonso, O.F., Loor, J.Y., Busto, R., and Ginsberg, M.D. (1999). Influence of early posttraumatic hypothermia therapy on local cerebral blood flow and glucose metabolism after fluid-percussion brain injury. J. Neurosurg. 90, 510–519.

Address correspondence to:
Neil G. Harris, M.D.
Department of Neurosurgery
David Geffen School of Medicine at UCLA
Box 957039
Los Angeles, CA 90095-7039

E-mail: ngharris@mednet.ucla.edu